CORE
Metadata, citation and similar papers at core.ac.uk
Provided by Sabanci University Research Database

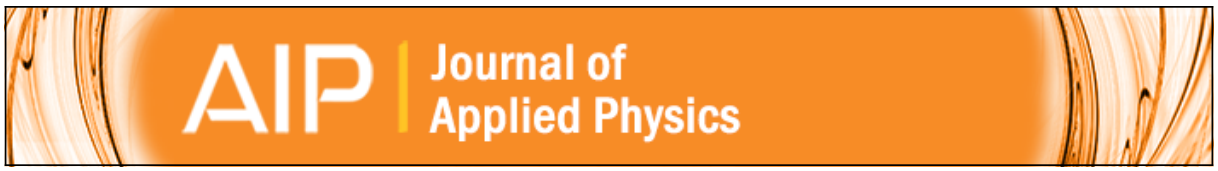

Very large dielectric response from ferroelectric nanocapacitor films due to collective surface and strain relaxation effects

I. B. Misirlioglu and M. Yildiz

Citation: Journal of Applied Physics **114**, 194101 (2013); doi: 10.1063/1.4831939
View online: http://dx.doi.org/10.1063/1.4831939
View Table of Contents: http://scitation.aip.org/content/aip/journal/jap/114/19?ver=pdfcov
Published by the AIP Publishing

Re-register for Table of Content Alerts

Create a profile.

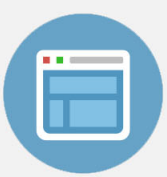

Sign up today!

[This article is copyrighted as indicated in the abstract. Reuse of AIP content is subject to the terms at: http://scitation.aip.org/termsconditions. Downloaded to] IP: 193.255.135.254 On: Tue, 03 Dec 2013 22:54:07

Very large dielectric response from ferroelectric nanocapacitor films due to collective surface and strain relaxation effects

I. B. Misirlioglu and M. Yildiz
Faculty of Engineering and Natural Sciences, Sabanci University, Orhanlı/Tuzla 34956 Istanbul, Turkey

(Received 23 September 2013; accepted 3 November 2013; published online 15 November 2013)

Dependence of the dielectric response of ferroelectrics on defect types, particularly those with long range strain fields in confined geometries have been often mentioned, especially in interpreting experimental results in films. However, detailed discussions on the mechanisms with which defects alter properties, particularly in the presence of interfaces imposing certain boundary conditions, are seldom made. Here, we studied the thickness dependence of transition temperatures and dielectric response of Metal/BaTiO3/Metal ferroelectric nanocapacitor structures grown on SrTiO3 using a phenomenological approach accounting for the equations of electrostatics and semiconductors. Relaxation of the misfit strain via misfit dislocations amplify the surface effects in films below a critical thickness and favor electrical domains leading to very large dielectric responses in this regime. Thin film structures with relaxed misfit strain in this work are fully depleted in the presence of moderate densities of impurities ($\sim 10^{25}$ m $^{-3}$). This is due to the reduction of polarization amplitude parallel to the film normal and its mplications for near-micron thick films are discussed. Consequently, the misfit dislocation sites have nearly no free carrier localization, making the role of these sites on leakage currents highly questionable. Dielectric response of intrinsic thicker films (>40 nm) is mostly under the influence of strain relaxation only with minimal interface impact in the limit of ideal electrodes. Our results point out that control of the dislocation density can lead to non-conventional functionalities in ferroelectric thin film capacitors via electromechanical coupling of properties to structure and domain stabilization. © *2013 AIP Publishing LLC*. [http://dx.doi.org/10.1063/1.4831939]

I. INTRODUCTION

Recently, a revived interest has arisen in defect related phenomena in ferroelectric structures including domain wall dynamics and their interaction with defects and charges,[1–16] driven by the demand for sustained functionality in reduced dimensions. Surfaces can also be treated as a type of defect where the crystal periodicity terminates, sometimes along with a local field.[17] In fact, surface boundary conditions and structural defects such as dislocations are thought to dominate nearly all the processes and functionality in a ferroelectric film during experiments or service in an application.[18–26] The way dislocations impact the properties is that they will mostly couple to the electrical properties rather indirectly through the polarization gradients or due to the inhomogeneous strain fields or electromechanically,[27] while the surfaces come into play via locally reduced paraelectric-ferroelectric transition temperatures (T_C), introduced by assigning polarization gradient a negative or a positive value, and electrostatic boundary conditions. For low-to-moderate magnitudes of lattice misfit between the film and the substrate (a few percent such as in the case of BaTiO3 and SrTiO3, which is about 2.5%, yielding a critical MD formation thickness of $\sim$ 3 nm), the effect of polarization divergence can be expected to become prominent in epitaxial thin films just above the critical thickness of MD formation where inhomogeneous strains will dominate. Such formations will also possibly smear the paraelectric-ferroelectric transition and associated anomalies in films near the critical thickness limit. The presence of a surface and its field component either originating from dangling bonds or absorbed species can smear the transition alone[17,18] and dependence of polarization orientation with respect to film surface due to sign of misfit strain at the phase transition has also been shown to smear out the dielectric anomaly.[19]

Depletion effects for low-to-moderate impurity densities can be neglected particularly in ultrathin films due to the relatively lower local electric field compared to the field formed emanating from a possible top-bottom electrode interface asymmetry, which we also demonstrated in a very recent work.[28] In real experiments, thin film capacitor samples hardly ever have symmetrical top-bottom interfaces due to processing sequence. Misfit dislocations (MDs) in a ferroelectric film might induce a similar effect due to the uneven strain distribution at top and bottom interfaces, possibly impacting nucleation and growth of domains under a given sign of applied bias voltage.[29,30] Structural defects, aside from what is mentioned above, have been corroborated as centers for the nucleation and pinning of domains during switching in addition to changing global strain states of films.[29–32] A strong correlation was observed experimentally between slip planes of dislocations and electrical domains in BTO[33] pointing out the impact of inhomogeneous strain fields on domain motion. Furthermore, a recent study reported that a regular domain pattern is stable only in the presence of defects that actually pin the domains.[34] Threading segments of the MDs were shown both theoretically and experimentally in the same year to pin switchable polarization and even cause

 © 2013 AIP Publishing LLC

[This article is copyrighted as indicated in the abstract. Reuse of AIP content is subject to the terms at: http://scitation.aip.org/termsconditions. Downloaded to] IP: 193.255.135.254 On: Tue, 03 Dec 2013 22:54:07

backswitching,[35,36] but this time not because of domain pinning but because of very high local T_C with abnormally high local coercive fields unresponsive to fields at the order of bulk coercive bias. Profound smearing of the phase transition can also occur due to presence of polarization gradients and inhomogeneity of the Curie-Weiss behavior even in the hypothetical case of infinite crystal with defects.[22,37]

When discussing the dielectric response, such as in this work, whether a single elastic domain will be stabilized or not upon dislocation formation is important and this apparently depends on the extent of self-strain. This was demonstrated recently in the work of Sheng *et al.* where their phase field simulations for PbTiO3 (PTO) yielded always a mixture of *c* and *a* domains near zero strain state in a thickness range not exceeding 30 nm.[38] Rhombohedral-tetragonal phase mixtures were predicted for $PbZr_{0.52}Ti_{0.48}O_3$ and $BiFeO_3$ under absence of electric field but this work considered homogeneous misfit strain relaxed only by domains.[39] For solid solutions of PTO-PbZrO3 in PTO rich stochiometries, a conclusion similar to that of Ref. 38 was reached previously in films with a homogenous background strain.[40] In case of $BaTiO_3$ (BTO), upon relaxation of the misfit with MDs, we find a monoclinic phase (also sometimes denoted as the *ac* phase) in all films far below the T_C especially for the 32 and 40 nm films. These films have an almost homogenous strain state away from the bottom interface where MDs exist. This outcome is in very good agreement with the misfit strain-temperature phase diagrams published in previous works due to the fact that these studies also considered homogeneous strains.[41–44] One must also note that some variances between these published results exist in the compressive strain part of the diagrams. Only at very small film thicknesses (less than 2 nm) is when significant deviation from these earlier published phase diagrams start according to Ref. 45 where a shift of the tetragonal phase to even relatively large tensile misfits was claimed. PTO on $SrTiO_3$ (STO) has been of special interest due to the small misfit between the two structures. A parallel result was obtained for PTO films on STO, justified by the Landau-Ginzburg formalism, where the coherent small lattice match above T_C turns into a tensile one upon paraelectric-ferroelectric transition and that the film still exists in tetragonal state[46] at very small thicknesses. A monodomain critical thickness of 14 nm was reported for PTO with a top free surface and that the free-surface charge was compensated via charge transfer leading to metallic layers on top.[47] These studies consider perfectly stoichiometric compositions without any MD relaxation. While carrying out the work, we felt the need to comment extensively on the effect of the extrapolation length on T_C and electrical domain stabilities as short extrapolation lengths (creating strong suppression of polarization at the interfaces) appear to have a direct and significant impact on the latter. Realistic extrapolation lengths (at the order of a few nm) can trigger electrical domain formation in the thermodynamic limit to confine the depolarizing electric field to the interface at the expense of domain wall energy, similar to the effect of dead layers and lead to very large dielectric response, a seldom mentioned point in previous works.

A sound understanding of the defect related effects on the properties of ferroelectric structures in reduced dimensions and with realistic boundary conditions is still under development and is of continued interest to interpret experimental results as well as new component designs. Here, we try to provide quantitative insight on the combined effect of MDs and surfaces on dielectric properties of thin film structures using a computational path in the continuum limit using the STO(substrate)/Metal/BTO/Metal (STO/M/BTO/M) thin film capacitor system as an example case. We focus on the changes in the transition temperature and dielectric response as a function of film thickness for an intrinsic state and with *n*-type impurities, which we consider to be oxygen vacancies donating electrons to the conduction band, within the wide bandgap semiconductor approach.[48] Due to the relaxation of the misfit strain with dislocations, we find an overall reduction in the polarization values, hence high dielectric constant, favoring full depletion in films with moderate impurity densities. This is quite different from what one would obtain for fully strained films under compressive misfit and leads us to think that unrelaxed films with enhanced T_C, hence probably polarization, could have partial depletion for relatively moderate-to-high impurity densities, making these structures more susceptible to leakage.

II. THEORY AND METHODOLOGY

The substrate-electrode-film-electrode system we consider is schematically depicted in Figure 1. The film is sandwiched between two electrodes that are pseudomorphic so that the film is directly under the influence of the structural misfit of the substrate. Once the film reaches a critical thickness, MDs with negative Burgers vector component along the film plane form at the bottom film-electrode interface in case of compressive misfit and a strain state with part of the misfit strain relieved in the film develops. This is the result of the MDs and the imaginary strain fields originating from the imaginary array of dislocations possessing mirror symmetry with the real ones with respect to the top film surface (Figure 1). We assume that $\vec{b} = a[\bar{1}00]$ type edge dislocations, following TEM studies on BTO/STO,[49,50] are stabilized right at the electrode-film interface (with the electrodes being fully coherent with the STO substrate) as to avoid complications due to the possibility that the MDs could

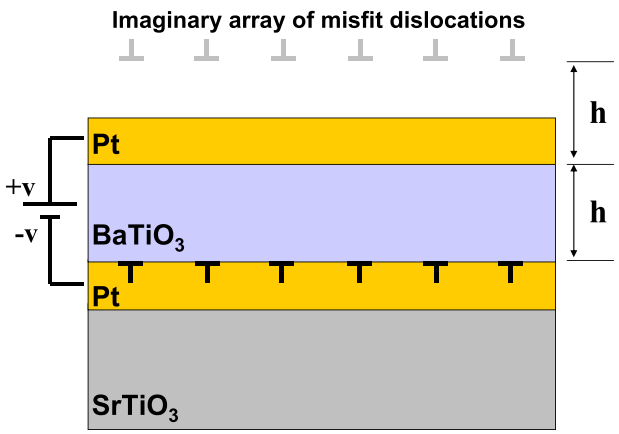

FIG. 1. The schematic of the STO/M/BTO/M system with MDs studied in this work.

[This article is copyrighted as indicated in the abstract. Reuse of AIP content is subject to the terms at: http://scitation.aip.org/termsconditions. Downloaded to] IP: 193.255.135.254 On: Tue, 03 Dec 2013 22:54:07

penetrate and stabilize within the less stiff electrode if thermal strains develop upon cooling after film growth.[51] The total strain, u^r_{ij}, at each coordinate in the film can be written as

$$u^r_{ij} = u^M_{ij} + u^D_{ij} + u^0_{ij}. \tag{1}$$

In Eq. (1), u^M_{ij} is the full biaxial in-plane misfit strain components between the film and the substrate in pseudocubic state given as $u^M_{ij} = (a_{subs} - a_{film})/a_{subs}$ where a_{subs} and a_{film} are the lattice parameters of the substrate and film, respectively, $u^0_{ij} = Q_{ijk}P^2_k$ is the self strain of the ferroelectric phase with Q_{ijk} being the electrostriction tensor, P_k is the ferroelectric polarization vector and we can drop this contribution out when discussing in-plane strain due to clamping on the substrate. u^D_{ij} is the relaxation by MDs via the normal strains (trace elements of the strain tensor). From here onwards, we only consider normal strains of MDs as these interact with the misfit strain. The normal strain component ($i = j$) due to a misfit dislocation array in a pseudocubic structure that relaxes the misfit strain at a coordinate $\vec{r}$ can be calculated in the general following form:

$$u^D_{ij} = \sum_{\varsigma=1} u^{\varsigma}_{ij}(1-\upsilon) + \upsilon u^{\varsigma}_{kk}\delta_{ij} + \sum_{\varsigma*=1} u^{\varsigma*}_{ij}(1-\upsilon) + \upsilon u^{\varsigma*}_{kk}\delta_{ij}. \tag{2}$$

u^D_{ij} is the total normal strain at a coordinate $\vec{r}$ in the film where ςdenotes summation of strains over the real dislocation array (first summation in Eq. (1)), ς^* denotes the summation of strains due to the imaginary dislocation array (second summation term in Eq. (1)), indices denote tensorial components wherein Einstein summation convention is enforced, δ_{ij} is the Kronecker delta. The imaginary component of MDs are such that the Burgers vector $\vec{b}^* = a[100]$ is the mirror operation in coordinates with respect to the top film surface to yield $\vec{b} * (x, y + 2h) = -\vec{b}(x, y)$ with x being the coordinate along the interface, y being the coordinate of the real dislocation along the vertical axis, h is the film thickness, a is the unitcell parameter of the film, υ in Eq. (2) is the Poisson ratio given as $-S_{12}/S_{11}$ where S_{ij} are the elastic compliances of BTO in the Voigt notation. The shear components of strain as well as the out-of-plane strain component are not considered due to the traction-free surface for the former and free expansion along z-axis for the latter, i.e., these components are stress-free strains (see Ref. 43). The individual normal dislocation strains that go into the summation in Eq. (2) are easily found from $u^{\varsigma}_{ij} = S_{ijkl}\sigma_{kl}$ in the usual definition where σ_{kl} are the well-known position dependent stress field components around an edge dislocation.[52] Thus, one can use an effective misfit strain as given y the first two terms in Eq. (1) at each coordinate in the film. Here, we consider 100 MDs symmetrically positioned with the periods obtained from Ref. 53 along the bottom film plane with respect to our computational domain such that the 51st MD site is at $x = 0$ with x varies from $-L/2$ to $L/2$ where L is the lateral length of the computational domain (200 nm here). The summed strain fields of the MDs gradually relax the misfit in our computational domain with increasing thickness. Note that this effective strain will be a function of coordinates in the film. The film satisfies the Maxwell Equation for dielectric media:

$$\nabla \cdot \vec{\mathbf{D}} = \rho, \tag{3}$$

where $\vec{\mathbf{D}} = D_x\vec{\mathbf{e}}_x + D_z\vec{\mathbf{e}}_z$, $D_x = \varepsilon_o\varepsilon_b E_x + P_x$ and $D_z = \varepsilon_o\varepsilon_b E_z + P_z$. Here, $\vec{\mathbf{D}}$ is the dielectric displacement vector, ε_o is the permittivity of vacuum, and ε_b is the background dielectric constant (7 in this work[54]), E_x and E_z are, respectively, the- and $z-$ components of the electric field vector $\vec{\mathbf{E}}$ determined from $E_x = -\partial\phi/\partial x$ and $E_z = -\partial\phi/\partial z$, P_x and P_z are the ferroelectric polarization components along x and z, respectively. ρ is the charge density in a n-type ferroelectric that consists of negative carriers in the conduction band, holes in the valence band and ionized impurities in the system expressed as

$$\rho = N^+_D + n^- + p^+, \tag{4}$$

for a semiconductor with only n-type impurities present. The terms in the right handside are

$$N^+_D = N_D(1 + g_D \exp[q(E_F - E_D - \phi)/kT])^{-1}, \tag{5a}$$

$$n^- = N_C(1 + \exp[q(E_C - E_F - \phi)/kT])^{-1}, \tag{5b}$$

$$p^+ = N_V(1 + \exp[q(E_F - E_V + \phi)/kT])^{-1}, \tag{5c}$$

where N_D is the donor impurity density, q is unit charge, E_F is the Fermi level (function of donor density, halfway of bandgap for intrinsic ferroelectric), E_D is the ionization energy of the n-type oxygen vacancy impurity in the crystal (taken with respect to te bottom of conduction band, 0,5 eV in our work for demonstrative purposes), ϕ is local electrostatic potential found from Eq. (3), N_C is the effective density of states in the conduction band, N_V is the effective density of states for holes in the valence band,E_V is the energy of the top of the valence band, g_D is the band degeneracy for a semiconductor (2 here), k is Boltzmann constant in eV units and T is temperature in Kelvin. In the case of intrinsic BTO, $\rho \cong 0$.

In the 2D limit, because of the symmetric film-plane equilibrium strain state, we consider only the strain term u^r_{11} that varies along the film thickness relaxing the misfit strain, u^M, which suffices for our purposes to demonstrate the inhomogeneous strain effects due to MDs (periodic MD segments are taken as infinite along the film plane). The strain fields and the charge distribution in the film are solved along with ferroelectric polarization, which has to satisfy the equations of state that are obtained via the variational minimization of the volumetric energy with respect to polarization components and the gradient of polarization:

$$\begin{aligned} &2\alpha^m_3 P_z + 4\alpha^m_{13}P_z P^2_x + 4\alpha^m_{33}P^3_z + 6\alpha_{111}P^5_z \\ &+\alpha_{112}(4P_z P^4_x + 8P^3_z P^2_x) + 2\alpha_{123}P_z P^4_x \\ &-G\left(\frac{\partial^2 P_z}{\partial z^2} + \frac{\partial^2 P_z}{\partial x^2}\right) = -\frac{\partial\phi}{\partial z}, \end{aligned} \tag{6a}$$

[This article is copyrighted as indicated in the abstract. Reuse of AIP content is subject to the terms at: http://scitation.aip.org/termsconditions. Downloaded to] IP: 193.255.135.254 On: Tue, 03 Dec 2013 22:54:07

$$2\alpha_1^m P_x + 2(2\alpha_{11}^m + \alpha_{12}^m)P_x^3 + 2\alpha_{13}^m P_x P_z^2 + 6\alpha_{111}P_x^5 + 2\alpha_{112}[3P_x^5 + 3P_x^3P_z^2 + P_xP_z^4] + 2\alpha_{123}P_x^3P_z^2 - G\left(\frac{\partial^2 P_x}{\partial z^2} + \frac{\partial^2 P_x}{\partial x^2}\right) = -\frac{\partial \phi}{\partial x}, \quad (6b)$$

where α_3^m, α_{13}^m, α_{33}^m, α_1^m, α_{11}^m, α_{12}^m are the renormalized dielectric stiffness coefficients in SI units with α_1^m and α_3^m containing the strain renormalization as $\alpha_1^m = \alpha(T - T_C) - (u_{ij}^M + u_{ij}^D)\ (Q_{11} + Q_{12})/(S_{11} + S_{12})$ and $\alpha_3^m = \alpha(T - T_C) - (u_{ij}^M + u_{ij}^D)2Q_{12}/(S_{11} + S_{12})$, $\alpha = (2\varepsilon_0 C)^{-1}$, α_{12}^m and α_{33}^m contain the clamping effect of the film, while α_{111}, α_{112}, and α_{123} are the dielectric stiffness coefficients in the bulk and can be found in Ref. 43. Thus, the Curie-Weiss terms of the equations of state are position dependent due to inhomogeneous total strain of MDs in Eq. (1). G is the gradient energy coefficient and is assumed to be isotropic for convenience, with a value of 6×10^{-10} m^3/F.[55] We solve Eqs. (4), (5), and (7) spontaneously in a numerical iterative scheme on a discrete grid with the top-bottom interface polarization boundary conditions given as

$$\lambda\frac{\partial P_x}{\partial x} - P_x = 0\Big|_{z=0,h} \quad \text{and} \quad \lambda\frac{\partial P_z}{\partial z} - P_z = 0\Big|_{z=z=0,h}, \quad (7)$$

with h being the film thickness, λ is the extrapolation length determining the extent of change of polarization along the film normal at the interface. Periodic boundary conditions are employed along the film plane both for polarization and electrostatic potential. Electrostatic boundary conditions at top-bottom film-electrodes are determined by the potential assigned to the electrodes ($\phi = \varphi \pm V_{app}/2$ at $z = 0, h$ where V_{app} is applied voltage, φ is the difference between the Fermi levels of the film and the electrode). The small signal dielectric response of the films is calculated from C-V simulations under the variation of a voltage signal applied as the boundary condition at the electrodes where the average dielectric displacements at the top interface (bottom can also be used) were computed and recorded both under zero bias and a small signal bias. The details are given in our recent work[28] and we do not repeat them here for brevity. Ideal metal electrodes are assumed whose work function is taken as that of Pt, a common electrode material (to determine electric boundary conditions at the electrodes), and the polarization charges at the interfaces are assumed to be completely screened. The constants used in the computation are provided in Table I. All our results are obtained at room temperature (RT).

TABLE I. Constants used in computing the semiconducting parameters (Vacuum level is reference and taken as zero).

E_F	E_D	E_V,	E_C	φ (Pt)	N_C	N_V
−5.1 eV (intrinsic)	−3.9 eV	−4.0 eV	−6.6 eV	−3.6 eV	−5.5 eV	10^{24}	10^{24}
(with impurities)						

III. RESULTS AND DISCUSSION

A. Intrinsic $BaTiO_3$

We computed the equilibrium misfit dislocation (MD) density (period) as a function of film thickness following the works given in Ref. 53 once the films are above the critical thickness (we calcuate this value to be around 3 nm for BTO on STO following the method in Ref. 56 where elastic constants given in Ref. 43 for BTO was used) and the result is provided in Figure 2. Using the MD periods pertaining to our cases, corresponding approximate pseudocubic film strain states ($u_{ij}^M + u_{ij}^D$ in Eq. (1)), we computed near the top interface of the films (where strain state tends to become homogeneous) in our study are given in secondary axis on the right. For comparison, we also give the "effective misfit" put forth in Ref. 53 and validate our results: There is excellent agreement (Figure 2(b)). As expected, thicker films gradually relax towards a zero strain state. With the core energy of MDs are being rather costly, the thinner films will have larger MD period while the thicker films, due to the high elastic strain energy, have smaller period, resulting in a relatively homogeneous strain state in the bulk of the film. The inhomogeneous strains around MD cores are confined to the bottom interface in the latter. The two cases create rather different conditions of polarization and domain stability as we shall show.

Before going onto the analysis of the dielectric response of the films, it is crucial to look at the paraelectric-ferroelectric transition temperatures, which we identified in cooling runs for the range of thicknesses considered here (Figure 3). Consistent with Figure 2, a near-full relaxation

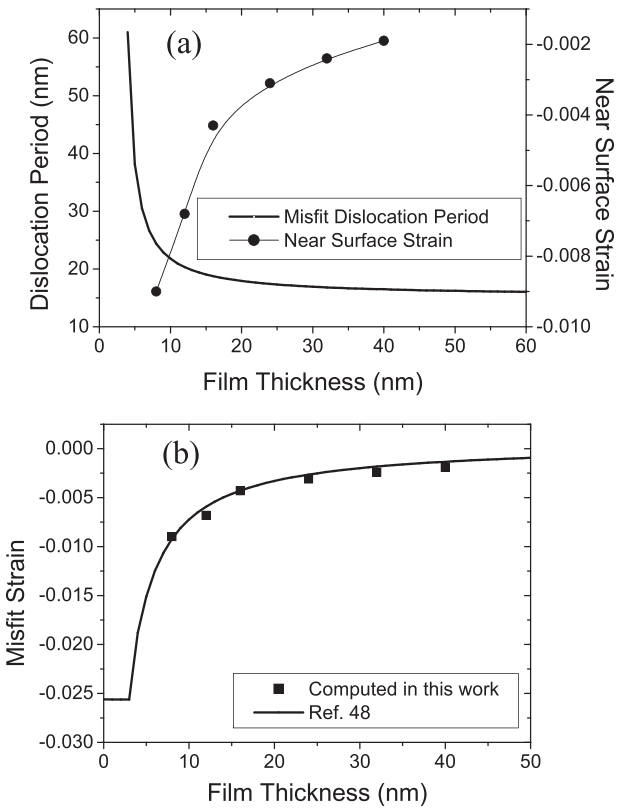

FIG. 2. (a) MD period vs. thickness computed using the formulation in Ref. 36 and strain vs. thickness computed for the given dislocation periods for the five thicknesses of films considered in this work, (b) Comparison of effective global strain defined in Ref. 47 with the computed data for the thicknesses considered in our work.

[This article is copyrighted as indicated in the abstract. Reuse of AIP content is subject to the terms at: http://scitation.aip.org/termsconditions. Downloaded to] IP: 193.255.135.254 On: Tue, 03 Dec 2013 22:54:07

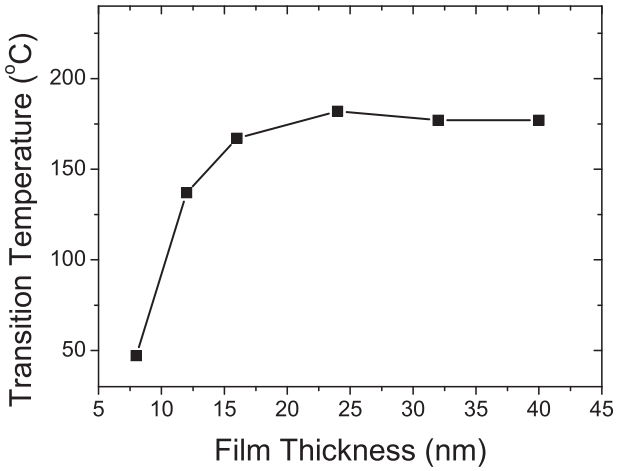

FIG. 3. Computed T_C as a function of thickness for the films considered in this work. Solid line is a guide to the eye.

state is achieved around 16 nm of thickness after which T_C remains nearly constant. The data in Figure 3 are extracted by tracking the absolute average amplitude of polarization ($\langle|P_Z|\rangle$) for films with domains the transition into multidomain state at T_C has zero average polarization and is not detectable if average of vector P_Z is tracked. For films having thickness < 20 nm with the equilibrium MD periods, we note that the multidomain and single domain energies are not very far apart and the considered extrapolation length, 3 nm, close to the values reported for such structures elsewhere,[57,58] favors the multidomain state owing to the electric fields forming near the surface. We check that it is so as bias fields at the order of 1/100 of the coercive fields can destabilize the multidomain state, which comes back following the removal of the bias. We also add here that the T_C reported for the films with MDs represent a transition from the paraelectric state into a monoclinic state, not tetragonal, which is bulk $BaTiO_3$ structure. Subsequently, a very interesting outcome of the thickness dependence of this transition is that thicker films (> 16 nm) exhibit abrupt changes in $\langle|P_x|\rangle$ as well as in $\langle|P_z|\rangle$ (due to coupling of the two). We find that these steps occur at temperatures close to T_C for the P_x component is necessary at the transition into multidomain state (forms right at T_C) in the form of closure domains while "strain stabilized" P_x component forms at lower temperatures, causing the jumps in amplitude. An example to such behavior is given Figure 4 along with the P_x component maps in the insets for the 32 nm film. Indeed, the temperature and strain (away from the bottom interface where near-homogeneous relaxation exists) at which structurally stable P_x appears in 32 and 40 nm films is in very good agreement with the temperature-misfit strain phase diagrams published previously[41–43] for small misfits (the results of these works vary at relatively large misfit strains with Refs. 41 and 43 being in close proximity).

The dielectric response of the films at various thicknesses and two different computed at RT for two different λ under small signal bias are plotted in Figure 5. In contrast to what is expected from Figure 3, the largest dielectric response is for the 16 nm film. The film with the lowest T_C for $\lambda = 3$nm is the 8 nm one and this structure is expected to

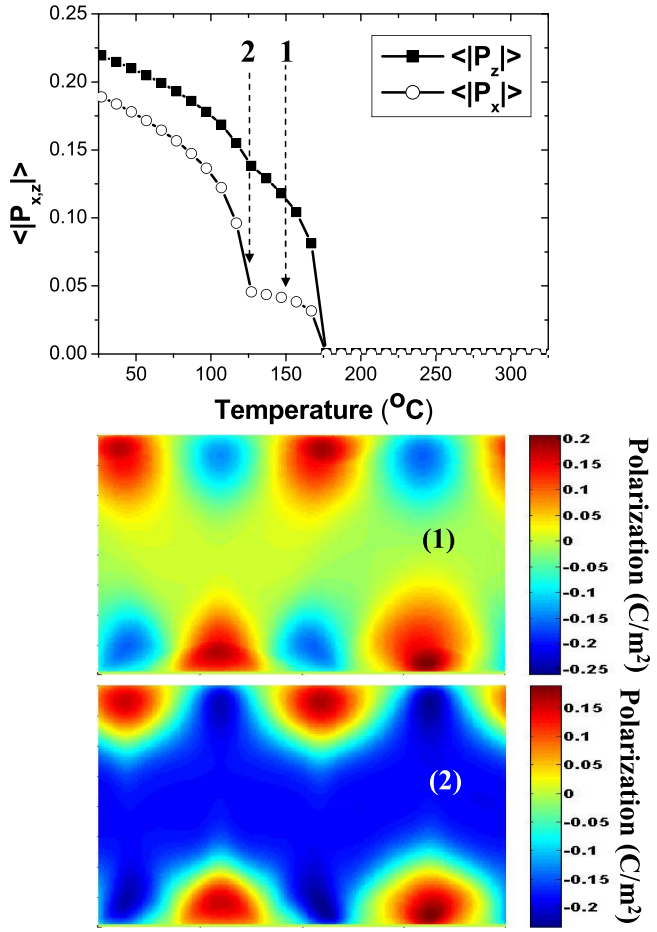

FIG. 4. $\langle|P_z|\rangle$ and $\langle|P_x|\rangle$ vs. temperature for the 32 nm thick film. 1 and 2 denote the amplitude maps of P_x at the temperatures indicated by the arrows.

exhibit a large dielectric response because T_C is closest to RT. Very thin films are expected to be under a strong influence of the surfaces as well as the inhomogeneous strain fields of the MDs. This statement is confirmed by the smeared transition for the 8 nm film (not shown here). MD density increases with thickness accompanied by a gradual decrease in the surface effect and a sharper T_C is observed for films thicker than 8 nm. Such a consequence originates from the fact that thicker films have the inhomogeneous strains due to MDs confined to the bottom interface, diminishing the smearing. We find that the large dielectric response for the 16 nm film is solely due to the presence of electrical domains, which is favored by the "partially relaxed misfit strains" in addition to the finite and small λ. A softer or susceptible P_z with respect to thicker films also promotes such behavior. Prediction of very large dielectric constants from multidomain films stabilized by thin dead layers at the film-electrode interfaces has been made sometime ago by Bratkovsky and Levanyuk[59] and the highest response would be attained if the domains are mobile, not pinned (which in their case was when dead layers at the film-electrode interfaces were very thin).

One can therefore conclude that relaxed ferroelectric nano film structures with realistic extrapolation lengths can exist in multidomain state and might generate very large

[This article is copyrighted as indicated in the abstract. Reuse of AIP content is subject to the terms at: http://scitation.aip.org/termsconditions. Downloaded to] IP: 193.255.135.254 On: Tue, 03 Dec 2013 22:54:07

dielectric responses, at the order a few thousand. Such an occurence is not the case for thicker films despite the fact that the misfit strain in these structures are nearly fully relaxed (see Figure 2). The dielectric response of 32 nm and 40 nm thick films is not different, implying the negligible surface effects in these structures and we find them to be in single domain state. A very informative demonstration supporting the argument related to the effect of extrapolation length above can be carried out. For this purpose, we computed the dielectric response of the same structures in the presence of very large extrapolation length (100 times the film thickness, $\lambda \cong \infty$), imposing nearly $dP_i/dx_i = 0$ at the surfaces as the polarization boundary condition (not to be confused with the electrical boundary conditions). The results are given in Figure 5 along with those obtained for $\lambda = 3$ nm. It is obvious that the trend for $dP_i/dx_i = 0$ at the surfaces is entirely consistent with the T_C given in Figure 2.

We also realize that, while the 8 nm film has the highest susceptibility to domain formation for $\lambda = 3$ nm, the 12 and 16 nm films are also in multidomain state with the latter two having a higher dielectric response in spite of the fact that they have higher T_C. We attribute this to the polarization magnitude in the individual domains. That the multidomain films with higher T_C are expected to have a higher dielectric response compared to those with lower T_C can be shown using the following rough but informative calculation. Let us assume that the polarization normal to the film plane in each domain of a multidomain ferroelectric film is homogeneous and we probe the linear dielectric response of such a system. Let us also consider that the dielectric response comes only from the z component of P, which is along the film normal (Homogeneously polarized closure domains have a small contribution and are constant within this approximation). The z-axis polarization (paralel to film normal) in direction of the field to be applied and the antiparallel polarization can be represented as $P_\uparrow$ and $P_\downarrow$, respectively. The changes in dielectric displacement will mostly depend on the change in ferroelectric polarization (due to the fact that the $\varepsilon_0\varepsilon_b E_Z$ term is negligibly smaller than P_z in Eq. (4)) and thus we write

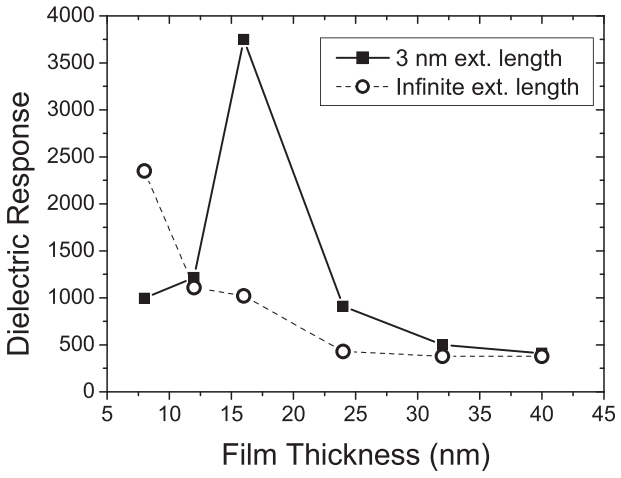

FIG. 5. Dielectric response as a function of thickness for $\lambda = 3$ nm and $\lambda = \infty$. The lines are guides for the eye.

$$D_i = \delta_\downarrow P_\downarrow + (1 - \delta_\downarrow)P_\uparrow, \tag{8}$$

for the initial dielectric displacement, D_i, at zero bias, neglecting the polarization of the domain walls and the closure domains which are smaller than the polarization in the domains themselves below T_C. Upon application of a small bias, ΔE, the final dielectric displacement, D_f, will become

$$D_f = (\delta_\downarrow - \Delta\delta)(P_\downarrow - \Delta P) + (1 - \delta_\downarrow + \Delta\delta)(P_\uparrow + \Delta P), \tag{9}$$

with $\Delta\delta$ and ΔP being the very small change in domain fraction and polarization due to applied small bias in the linear limit. Because we probe linear response at small bias, ΔP is the same both in paralel and antiparallel directions and is always positive. Note that $P_\downarrow$ and $P_\uparrow$ are vectors and have opposite signs. From the definition of dielectric response, $\varepsilon_r = (1/\varepsilon_0)dD/dE$, one obtains from $\varepsilon_r = (1/\varepsilon_0)(D_f - D_i)/\Delta E$ the following:

$$\varepsilon_r \propto \Delta\delta(P_\uparrow - P_\downarrow) + \Delta P(1 + 2\Delta\delta - 2\delta_\downarrow) \tag{10}$$

and noting that $\delta_\downarrow = 0.5$ initially, one has

$$\varepsilon_r \propto \Delta\delta(P_\uparrow - P_\downarrow) + 2\Delta P\Delta\delta. \tag{11}$$

In Eq. (11), the first term is the multidomain response (Remember that $P_\uparrow - P_\downarrow \cong 2P_S$ where P_S is approximately the spontaneous polarization in single domain state for a film with a given T_C) while the second term is important only very close to or at T_C where the system is highly sensitive to infinitesmally small perturbations. Thus, below T_C, the first term dominates the dielectric response. According to Eq. (11), a multidomain film with a lower T_C is expected to have a lower dielectric response with respect to a multidomain film with higher T_C. Inserting the average polarization values for $P_{\downarrow,\uparrow}$ we obtained from our simulations into Eq. (11), we indeed see that the 16 nm film, for instance, is expected to have a dielectric response higher than the 8 and 12 nm ones, although we cannot quantify the roughly 3 times difference due to the approximate nature of the approach presented above. Another fact is that the thinner films will probably have reduced domain wall mobility due to the stronger depolarizing fields penetrating to a significant volume of the film (making domain walls more stable hence "harder" to move), meaning smaller $\Delta\delta$, rendering a lower dielectric response expectation. Note that without pinning either due to MDs or value of λ, one might actually have much larger responses than what we report here but in real experiments one should always expect pinning of domains. In the approximate model prescribed above, it is also easy to see that the single domain dielectric response can be recovered using Eq. (10) if one takes $P_\downarrow = 0, \delta = 1$ and $\Delta\delta = 0$. Then one is left only with $(1/\varepsilon_0)\Delta P/\Delta E$ which is just the dielectric response of a homogeneous single domain film that diverges at T_C in accordance with the Curie-Weiss behavior.

Films with 24, 32, and 40 nm thickness in this work sustain single domain states (or it can be said that the single domain and multidomain energies are very close) and the dielectric response we get from these structures are nearly

[This article is copyrighted as indicated in the abstract. Reuse of AIP content is subject to the terms at: http://scitation.aip.org/termsconditions. Downloaded to] IP: 193.255.135.254 On: Tue, 03 Dec 2013 22:54:07

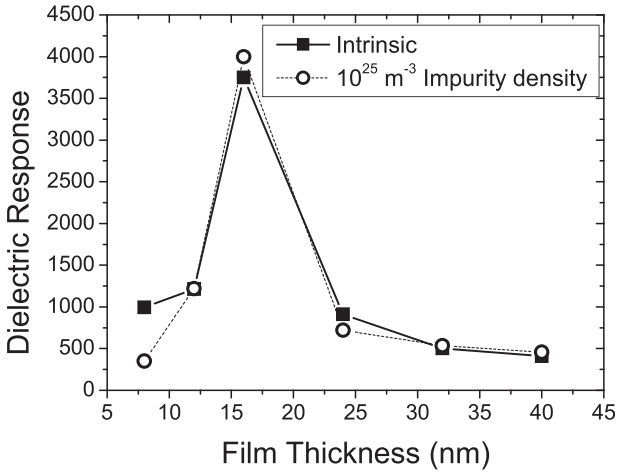

FIG. 6. Dielectric response as a function of thickness for intrinsic BTO and BTO with $10^{25}\,m^{-3}$ impurity density. $\lambda = 3nm$ in both cases.

the same as the case of infinite extrapolation length. Therefore, one can conclude that the response of thicker structures are determined by the extent of strain relaxation by the MDs, the polarization boundary conditions at the interfaces is of secondary importance.

B. $BaTiO_3$ with moderate impurity density

The inclusion of the semiconducting properties to account for depletion charges emanating from the ionizable impurities do not have a significant impact on the dielectric response. For films with impurity density of $10^{25}\,m^{-3}$ (values close to this have been reported for such systems) we obtained nearly the same behavior as the intrinsic films. Results are provided in Figure 6 in comparison with the intrinsic BTO film. Another important aspect to consider is the coupling of the inhomogenous dislocation fields to free carrier and ionized impurity distribution. This happens via the divergence of ferroelectric polarization term of the dielectric displacement in Eq. (3). Due to the strain relaxation caused by MDs, the magnitude of P_z normal to the film-electrode interface is lower compared to a fully strained film and this diminishes the effect of the polarization on depletion charge distribution. This is mainly the mechanism by which dislocation straşn fields act on the depletion charge and carrier distribution. Therefore, along with the increased dielectric constant owing to relaxed misfit strain, the films are all fully depleted and they remain so even for densities around $10^{26}\,m^{-3}$ (not shown). Hence, there is only ionized, positively charged impurities in the films and nearly no free carriers including dislocation sites. The thicker films have a very slightly enhanced dielectric response and this is because of the slightly reduced P_z due to the higher magnitude of the internal electric field changing sign in the middle of the film along thickness as also discussed elsewhere.[60] This outcome of our study has very important implications for the tempting thought that films with MDs might be more prone to leakage compared to films with fully coherent interfaces with the underlying substrate. As the films are fully depleted, we did not find any carrier localization around MD sites. Importance of such a finding lies in the fact that width of the depletion zones near the electrodes in ferroelectric semiconductors with impurities is an important parameter when discussing leakage and charge injection as the electric field distribution inside the films with partial and full depletion are very different, impacting the maximum electric field at the interfaces. Interface fields directly determine the threshold for electron emission from the electrode over a barrier characteristics in such systems and is of ultimate importance for device funcitonality. The threading segments of the MDs, on the other hand, need to be considered seperately as they are often thought as conducting pathways between upper and bottom electrodes under applied bias.

IV. CONCLUSIONS

We simulated the transition temperatures and dielectric response of STO/Metal/BTO/Metal thin film structures for various thickness of the BTO layer in the presence strain relaxation via MDs, connecting effect of microstructural features to macroscopic response. All films were computed to be in the monoclinic phase. Both the intrinsic films and films with impurities display a very large dielectric response around a critical thickness where the strain relaxation amplifies the impact of the surface. For very thin films, the dielectric response is more pronunced due to the combined effect of surface boundary conditions and the inhomogeneous MD strain fields occupying a very significant volume of the film stabilizing electrical domains. Using a simple model, we confirmed the trends of the simulations for realistic extrapolation lengths where the multidomain films with higher T_C are expected to have a larger dielectric response than those multidomain films with lower T_C. Putting an infinite extrapolation length removes any polarization-related surface effect and films attain a single domain dielectric response in proportion with the T_C determined by MD density. For realistic extrapolation lengths films above a certain thickness, despite near-full relaxation with MDs, can sustain a single domain state and these structures still have a pronounced dielectric response due to polarization instabilities around dislocation cores in addition to the existence of the monoclinic state. Moderate amounts of depletion charge do not change the trends we observe in the intrinsic films. Due to the reduced polarization magnitude along the film normal, all films studied here are in full-depletion state with nearly no density of free carriers, revealing an effective mechanism by which dislocations determine carrier distribution in the film. No special or preferential distribution of free carriers was observed around MD cores, leading us to the idea that polarization gradients do not have a profound effect on free charge distribution or localization as one might be compelled to think as long as the film thickness allows fully depleted state. This scenario might change for sufficiently thick films that will be in partial depletion for the reported densities of impurities in literature. Moreover, the assumption that impurity generated carriers can compensate for local electric fields due to polarization gradients remains formally invalid for films with moderate amounts of impurities as these films will be in fully depleted state. We did not come across a systematic experimental study of the thickness dependence of dielectric

[This article is copyrighted as indicated in the abstract. Reuse of AIP content is subject to the terms at: http://scitation.aip.org/termsconditions. Downloaded to] IP: 193.255.135.254 On: Tue, 03 Dec 2013 22:54:07

response of high quality epitaxial BTO films on compressive substrates for comparison of our findings and we hope that the current paper might motivate such a work to clarify MD effects in particular. A careful systematic work on a wide range of thicknesses with high quality films was carried out in Ref. 61, but the system analyzed there was $Ba_{0.5}Sr_{0.5}TiO_3$ on MgO under a finger electrode geometry, rendering the associated polarization stabilities, domain structures and electrostatics incomparable to the predictions of our work.

ACKNOWLEDGMENTS

I.B.M. acknowledges the support of Turkish Academy of Sciences (TUBA) GEBIP.

[1]P. Gao, C. T. Nelson, J. R. Jokisaari, S. H. Baek, C. W. Bark, Y. Zhang, E. G. Wang, D. G. Schlom, C. B. Eom, and X. Q. Pan, Nat. Commun. **2**, 591 (2011).
[2]C. T. Nelson, P. Gao, J. R. Jokisaari, C. Heikes, C. Adamo, A. Melville, S. H. Baek, C. M. Folkman, B. Winchester, Y. J. Gu, Y. M. Liu, K. Zhang, E. G. Wang, J. Y. Li, L. Q. Chen, C. B. Eom, D. G. Schlom, and X. Q. Pan, Science **334**, 968 (2011).
[3]S. M. Yang, J. G. Yoon, and T. W. Noh, Curr. Appl. Phys. **11**, 1111 (2011).
[4]A. Oubelkacem, I. Essaoudi, A. Ainane, M. Saber, and F. Dujardin, Phys. Scr. **83**, 055704 (2011).
[5]D. Kedzierski, E. V. Kirichenko, and V. A. Stephanovich, Phys. Lett. A **375**, 685 (2011).
[6]R. A. Kraya and L. Y. Kraya, J. Appl. Phys. **112**, 123708 (2012).
[7]A. V. Kimmel, P. M. Weaver, M. G. Cain, and P. V. Sushko, Phys. Rev. Lett. **109**, 117601 (2012).
[8]C. R. Winkler, M. L. Jablonski, A. R. Damodaran, K. Jambunathan, L. W. Martin, and M. L. Taheri, J. Appl. Phys. **112**, 052013 (2012).
[9]H. Zhou, J. W. Hong, Y. H. Zhang, F. X. Li, Y. M. Pei, and D. N. Fang, Physica B **407**, 3377 (2012).
[10]D. Wang, X. Q. Ke, Y. Z. Wang, J. Gao, H. Y. Wang, L. Zhang, X. S. Yang, and X. B. Ren, Phys. Rev. B **86**, 054120 (2012).
[11]P. Paruch, A. B. Kolton, X. Hong, C. H. Ahn, and T. Giamarchi, Phys. Rev. B **85**, 214115 (2012).
[12]A. S. Sidorkin, L. P. Nesterenko, and A. Y. Pakhomov, Phys. Solid State **54**, 1008 (2012).
[13]N. C. Bristowe, M. Stengel, P. B. Littlewood, J. M. Pruneda, and E. rtacho, Phys. Rev. B **85**, 024106 (2012).
[14]A. Pramanick, A. D. Prewitt, J. S. Forrester, and J. L. Jones, Crit. Rev. Solid State Mater. Sci. **37**, 243 (2012).
[15]L. Gunawan, G. Z. Zhu, Y. Shao, S. Laza, O. Gautreau, C. Harnagea, A. Pignolet, and G. A. Botton, J. Appl. Phys. **113**, 044102 (2013).
[16]E. A. Eliseev, P. V. Yudin, S. V. Kalinin, N. Setter, A. K. Tagantsev, and A. N. Morozovska, Phys. Rev. B **87**, 054111 (2013).
[17]A. M. Bratkovsky and A. P. Levanyuk, Phys. Rev. Lett. **94**, 107601 (2005).
[18]S. Bin-Omran, I. Kornev, I. Ponomareva, and L. Bellaiche, Phys. Rev. B **81**, 094119 (2010).
[19]A. K. Tagantsev, N. A. Pertsev, P. Muralt, and N. Setter, Phys. Rev. B **65**, 012104 (2002).
[20]C. L. Canedy, H. Li, S. P. Alpay, L. Salamanca-Riba, A. L. Roytburd, and R. Ramesh, Appl. Phys. Lett. **77**, 1695 (2000).
[21]M.-W. Chu, I. Szafraniak, R. Scholz, C. Harnagea, D. Hesse, M. Alexe, and U. Gösele, Nature Mater. **3**, 87 (2004).
[22]R. Skulski and P. Wawrzala, Physica B **233**, 173 (1997).
[23]S. Y. Hu, Y. L. Li, and L. Q. Chen, J. Appl. Phys. **94**, 2542 (2003).
[24]G. Akcay, I. B. Misirlioglu, and S. P. Alpay, J. Appl. Phys. **101**, 104110 (2007).
[25]W. K. Simon, E. K. Akdogan, A. Safari, and J. A. Bellotti, Appl. Phys. Lett. **87**, 082906 (2005).
[26]F. Ludwig, I. B. Misirlioglu, I. Vrejoiu, M. Alexe, and D. Hesse, J. Appl. Phys. **105**, 061607 (2009).
[27]D. Balzar, P. A. Ramakrishnan, and A. M. Hermann, Phys. Rev. B **70**, 092103 (2004).
[28]I. B. Misirlioglu and M. Yildiz, J. Phys. D: Appl. Phys. **46**, 125301 (2013).
[29]S. V. Kalinin, B. J. Rodriguez, A. Y. Borisevich, A. P. Baddorf, N. Balke, H. J. Chang, L. Q. Chen, S. Choudhury, S. Jesse, P. Maksymovych, M. P. Nikiforov, and S. J. Pennycook, Adv. Mater. **22**, 314 (2010).
[30]P. Maksymovych, N. Balke, S. Jesse, M. Huijben, R. Ramesh, A. P. Baddorfi, and S. V. Kalinin, J. Mater. Sci. **44**, 5095 (2009).
[31]L. W. Chang, M. McMillen, and J. M. Gregg, Appl. Phys. Lett. **94**, 212905 (2009).
[32]Y. L. Li, S. Y. Hu, S. Choudhury, M. I. Baskes, A. Saxena, T. Lookman, Q. X. Jia, D. G. Schlom, and L. Q. Chen, J. Appl. Phys. **104**, 104110 (2008).
[33]D. Liu, D. Chelf, and K. W. White, Acta Mater. **54**, 4525 (2006).
[34]M. Y. Gureev, P. Mokry, A. K. Tagantsev, and N. Setter, Phys. Rev. B **86**, 104104 (2012).
[35]I. B. Misirlioglu, S. P. Alpay, M. Aindow, and V. Nagarajan, Appl. Phys. Lett. **88**, 102906 (2006).
[36]I. Vrejoiu, G. Le Rhun, N. D. Zakharov, D. Hesse, L. Pintilie, and M. Alexe, Philos. Mag. **86**, 4477 (2006).
[37]A. P. Levanyuk and A. S. Sigov, "Defects and Structural Phase Transitions," in *Ferroelectricity and Related Phenomena*, edited by W. Taylor (Gordon and Breach Science Publishers, 1988), Vol. 6.
[38]G. Sheng, J. M. Hu, J. X. Zhang, Y. L. Li, Z. K. Liu, and L. Q. Chen, Acta Mat. **60**, 3296 (2012).
[39]J. Ouyang, W. Zhang, X. Y. Huang, and A. L. Roytburd, Acta Mater. **59**, 3779 (2011).
[40]Q. Y. Qiu, R. Mahjoub, S. P. Alpay, and V. Nagarajan, Acta Mater. **58**, 823 (2010).
[41]V. B. Shirokov, Yu. I. Yuzyuk, B. Dkhil, and V. V. Lemanov, Phys. Rev. B **75**, 224116 (2007).
[42]I. B. Misirlioglu, S. P. Alpay, F. He, and B. Wells, J. Appl. Phys. **99**, 104103 (2006).
[43]N. A. Pertsev, A. G. Zembilgotov, and A. K. Tagantsev, Phys. Rev. Lett. **80**, 1988 (1998).
[44]O. Dieguez, S. Tinte, A. Antons, C. Bungaro, J. B. Neaton, K. M. Rabe, and D. Vanderbilt, Phys. Rev. B **69**, 212101 (2004).
[45]J. Paul, T. Nishimatsu, Y. Kawazoe, and U. V. Waghmare, Phys. Rev. Lett. **99**, 077601 (2007).
[46]D. D. Fong, G. B. Stephenson, S. K. Streiffer, J. A. Eastman, O. Auciello, P. H. Fuoss, and C. Thompson, Science **304**, 1650 (2004).
[47]J. He, G. B. Stephenson, and S. M. Nakhmanson, J. Appl. Phys. **112**, 054112 (2012).
[48]Y. Xiao, V. B. Shenoy, and K. Bhattacharya, Phys. Rev. Lett. **95**, 247603 (2005).
[49]H. P. Sun, W. Tian, X. Q. Pan, J. H. Haeni, and D. G. Sclom, Appl. Phys. Lett. **84**, 3298 (2004).
[50]T. Suzuki, Y. Nishi, and M. Fujimoto, Philos. Mag. A **79**, 2461 (1999).
[51]It was experimentally observed that misfit dislocations can penetrate into the softer electrode upon forming probably during cooling where thermal stresses develop: V. Nagarajan, C. L. Jia, H. Kohlstedt, R. Waser, I. B. Misirlioglu, S. P. Alpay, and R. Ramesh, Appl. Phys. Lett. **86**, 192910 (2005).
[52]J. P. Hirth and J. Lothe, *Theory of Dislocatons*, 2nd ed. (Wiley, New York, 1982).
[53]J. S. Speck and W. Pompe, J. Appl. Phys. **76**, 466 (1994); S. P Alpay and A. L. Roytburd, *ibid.* **83**, 4714 (1998).
[54]J. Hlinka and P. Marton, Phys. Rev. B **74**, 104104 (2006); A. K Tagantsev, Ferroelectrics **375**, 19 (2008).
[55]Please see the Appendix in A. M. Bratkovsky and A. P. Levanyuk, J. Comput. Theor. Nanosci. **6**, 465 (2009).
[56]W. D. Nix, Metall. Trans. A **20**, 2217 (1989).
[57]V. Nagarajan, S. Prasertchoung, T. Zhao, H. Zheng, J. Ouyang, R. Ramesh, W. Tian, X. Q. Pan, D. M. Kim, C. B. Eom, H. Kohlstedt, and R. Waser, Appl. Phys. Lett. **84**, 5225 (2004).
[58]C. Jia, V. Nagarajan, J. He, L. Houben, T. Zhao, R. Ramesh, K. Urban, and R. Waser, Nat. Mater. **6**, 64 (2007).
[59]A. M. Bratkovksy and A. P. Levanyuk, Phys. Rev. B **63**, 132103 (2001).
[60]I. B. Misirlioglu, H. N. Cologlu, and M. Yildiz, J. Appl. Phys. **111**, 064105 (2012).
[61]H. Li, A. L. Roytburd, S. P. Alpay, T. D. Tran, L. Salamanca-Riba, and R. Ramesh, Appl. Phys. Lett. **78**, 2354 (2001).

[This article is copyrighted as indicated in the abstract. Reuse of AIP content is subject to the terms at: http://scitation.aip.org/termsconditions. Downloaded to] IP: 193.255.135.254 On: Tue, 03 Dec 2013 22:54:07